We are IntechOpen, the world's leading publisher of Open Access books Built by scientists, for scientists

4,800
Open access books available

122,000
International authors and editors

135M
Downloads

Our authors are among the

154
Countries delivered to

TOP 1%
most cited scientists

12.2%
Contributors from top 500 universities

WEB OF SCIENCE™

Selection of our books indexed in the Book Citation Index in Web of Science™ Core Collection (BKCI)

Interested in publishing with us?
Contact book.department@intechopen.com

Numbers displayed above are based on latest data collected.
For more information visit www.intechopen.com

Chapter

Importance of Surface Energy in Nanoemulsion

Kaustav Bhattacharjee

Abstract

The emerging prospects of nanoscience and nanotechnology have an enormous promise to revolutionize various aspects of human life. In this context, the application of nanoemulsion stands at the vanguard of introducing newer dimensions to the way we see the everyday world. Naturally, the preparation and stability of nanoemulsion demand a precise understanding of the underlying forces of interaction toward achieving a greater control over their functionality and regulating them. The stability of nanoemulsion is primarily governed by the conjugate and complex interplay of van der Waals forces and steric interactions. The present chapter will be dedicated to the discussion of the regulatory roles of these forces in dictating the stability of nanoemulsion with particular emphasis on the origin of these fundamental forces from a molecular-level viewpoint.

Keywords: surface tension, curvature, Ostwald ripening, steric stabilization

1. Introduction

An emulsion is a special form of colloid where one liquid (dispersed phase) is uniformly distributed in another liquid (dispersion matrix) [1, 2]. Minute droplets of dispersed phase which is otherwise immiscible in the dispersion medium form a statistically distributed system encapsulated within the matrix having a boundary between the phases, called the "interface." Oil (O), water (W) and surfactants (S) are the three key components of the emulsion. Depending on the order of preparation, it can be water in oil (W/O), oil in water (O/W), water in oil in water (W/O/W), or oil in water in oil (O/W/O) [1]. In view of the interest of the present discussion, we will focus only on O/W emulsion throughout the chapter. O/W emulsion consists of small globular compartments composed of oil (lipophilic) and surfactant which can be conveniently dispersed in water.

Such system has a great deal of research interest in the field of food, pharmaceutical, agrochemical and other industries with certain benefits ([3–5] and references therein). *First*, they usually have improved stability to particle aggregation and eventual sedimentation. *Second*, by virtue of the appropriate small size of the droplets, they only weakly scatter light wave and therefore are advantageous for adding values into the products that need to be optically transparent (or only slightly turbid). *Third*, they can be tailor made to have novel rheological properties. *Fourth*, they have a much higher bioavailability of specific types of bioactive molecules contained within the dispersed phase.

Due to the fact that the environment of a molecule at an interface is different than those of the bulk phase, an interface is always associated with surface free

energy. The free energy per unit area, measured in terms of the surface tension (γ), is the minimum amount of work required to create a new area of that interface [6]. Minimization of the interfacial contact area is therefore a spontaneous process. A surface-active agent (or surfactant) is a substance which at low concentration can adsorb at the interface, thereby reducing the amount of work required to expand it [7, 8]. In general, surfactants are amphiphilic molecules which reduce the interfacial surface tension due to their dual chemical nature and strong tendency to self-assemble above a certain concentration (precisely a narrow concentration range) at a given temperature, known as the critical micellar concentration (CMC). There are two most common types of emulsion classified in the literature based on their stability and structural components, namely, *microemulsion* and *nanoemulsion* [3]. Both types have droplet radius in the range of sub-100 nanometers. Despite several dissimilarities between these two kinds, it has been unfortunate that there has been a great confusion and widespread errors in their usage in the scientific literature. The confusion comes from the prefixes used to denote them. As the terms "micro-" (10^{-6}) and "nano-" (10^{-9}) suggest, it is assumed that nanoemulsions contain droplets that are smaller than microemulsion. In practice, the opposite is often found; indeed, there has also been much disagreement about the critical droplet size to distinguish between the two. A clear distinction between these two types of liquid-in-liquid dispersion has been made in two recent studies [3, 4], and the interested readers are suggested to go through the references. However, a brief clarification is given in the present chapter.

A free energy diagram for the two systems is schematically shown in **Figure 1**. An O/W-type microemulsion is a thermodynamically stable isotropic dispersion of oil and surfactant in water. Nevertheless, it is strongly affected and even broken up by modulations in thermodynamic variables, such as temperature, composition, pH, etc. Microemulsions are formed spontaneously (without the need of an external agency) when surfactants are added to the oil-water mixture [3, 4]. The non-polar tails of surfactant molecules self-assemble to form a hydrophobic core where oil molecules can be stored and separated from the thermodynamically unfavorable aqueous phase of the surroundings. The final structure of such microenvironment may result in a spherelike (micelle or reverse micelle), cylinder-like (rod micelle), plane-like (lamellar micelle) or sponge-like (bicontinuous) shape.

On the other hand, an O/W-type nanoemulsion is a thermodynamically unstable isotropic dispersion of oil and surfactant in water [3, 4]. In principle, nanoemulsion

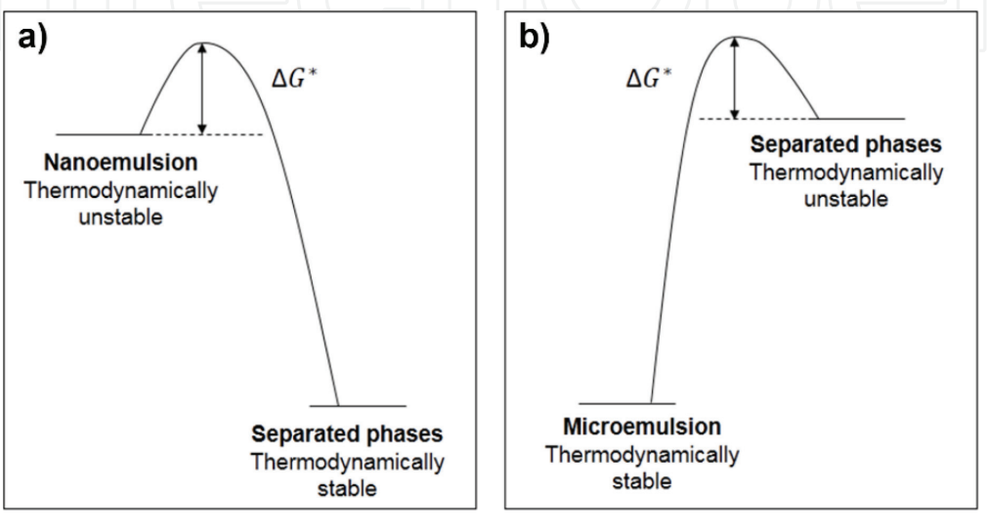

Figure 1.
Schematic diagram of the free energy of (a) nanoemulsion and (b) microemulsion system in comparison to their respective reference states. The two states are separated by an activation energy ΔG.*

can be fabricated without addition of any surfactant molecule only by physical methods that involve energy input. However, such a system would be highly unstable with respect to droplet coalescence (merging of two droplets) and phase segregation. Therefore, surfactant is needed to ensure the kinetic stability of nanoemulsion during prolonged storage [8]. Nevertheless, under certain circumstances surfactant may impart negative effect on nanoemulsion stability, because of their ability to enhance the mass transfer processes which can cause significant change in droplet concentration, composition and size distribution [8]. The mass transport process is typically driven by differences in chemical potentials for the solutes in each microenvironment, and as a consequence, droplets tend to merge and transport the dissolved matter through the dispersion medium, by a process known as "Ostwald ripening." Another essential difference between micro- and nanoemulsion that is often neglected in the literature is the influence of the order in which different compounds are mixed together during preparation [3]. This point is particularly important for nanoemulsion. Nanoemulsions are only formed if the surfactants are first mixed with the oil phase and then the surfactant-oil mixture is added to the aqueous phase. If it is not followed, only a "macroscopic" emulsion will be generated. Microemulsion, on the contrary, will be strictly identical whatever the order in which the components are mixed (after equilibrium time).

The major advantages and disadvantages of nanoemulsion over microemulsion for the specific application purpose are summarized below [3, 4].

1.1 Advantages

(1) Due to their smaller droplet size, reduction under gravitational pull can be avoided in large extent, and, therefore, nanoemulsion never shows creaming and sedimentation problems, while these problems are quite common with conventional emulsion or even with microemulsion. With proper stabilization forces, nanoemulsions can be stored for a longer period than microemulsion. (2) Nanoemulsions are very suitable for rapid penetration of active ingredients (pharmaceuticals and/or food) due to their smaller size and large surface area. (3) Unlike microemulsion which requires high surfactant concentration (20% or higher), nanoemulsion can be formed using reasonably low surfactant concentration (5–10%).

1.2 Disadvantages

(1) Fabrication of nanoemulsion in many cases demands special and expensive instrumentation (high-pressure homogenizers or ultrasonics, microfluidizer, etc.), technique as well as higher concentration of surfactants. (2) The lacuna in the understanding of various fundamental issues associated with nanoemulsion strongly restricts its acceptability and applicability. Knowledge of proper interfacial chemistry, mechanism of Ostwald ripening and ingredients to overcome it are the key issues that need to be taken care of for the superior acceptability and applicability of nanoemulsion.

2. Thermodynamics and kinetics of nanoemulsion

2.1 Free energy diagram

The thermodynamic stability of a particular system is governed by the change in free energy between it and an appropriate reference state. Nanoemulsion is thermodynamically unstable, which means that the free energy of nanoemulsion is

higher than the free energy of the separate phases (oil and water). For microemulsion, this condition is opposite. To understand the molecular basis of the free energy difference, let us consider that a system (nano-/microemulsion) exists in equilibrium between the initial and final states. The free energy change associated with the formation of the dispersion consists of an interfacial free energy term (ΔG_I) and a configuration entropy term ($-T\Delta S_{config}$) [9]:

$$\Delta G_{formation} = \Delta G_I - T\Delta S_{config}.$$

The free energy to increase the contact area (ΔA) at the interface is $\Delta G_I = \gamma \Delta A$, which is always positive; consequently, this term always opposes the formation of the dispersions. However, the interfacial tension (γ) depends on the curvature of the surfactant layer-decreasing as the curvature approaches to its optimum value. A phenomenological description of the dependence of interfacial tension on droplet curvature can be formulated as [10–12]:

$$\gamma = \gamma_0 + (\gamma_\infty + \gamma_0)\frac{(R_0 - R)^2}{R_0^2 + R^2},$$

where γ_∞ and γ_0 are, respectively, the interfacial tension values at the planar O/W interface and when the surfactant layer reaches its optimum curvature. R_0 is the droplet radius at the optimum curvature.

On the other hand, configuration entropy (ΔS_{config}) which depends on the number of arrangements accessible to the oil phase in an emulsified state is much greater than that in a non-emulsified state, and therefore it always favors the formation of the dispersion. An expression for the ΔS_{config} can be derived from the statistical analysis [9]:

$$\Delta S_{config} = -\frac{nk}{\phi}(\phi ln\phi + (1-\phi)\ln(1-\phi)),$$

where k is the Boltzmann constant, n is the number of droplets and ϕ is the disperse-phase volume fraction.

The plot for the different free energies with droplet radius assuming that the interfacial tension is the same as that for planer O/W interface is shown in **Figure 2(a)** [3]. It can be observed from the figure that the interfacial free energy contribution increases (hence unfavorable) with decrease in droplet size (increase in interfacial area), while the configuration of free energy becomes progressively negative (hence favorable) with decrease in droplet size (increase in number of different ways that droplet can be organized). The total free energy, however, becomes increasingly positive with decrease in droplet size, since the interfacial free energy term dominates the configuration entropy term.

This implies that the formation of nanoemulsion becomes increasingly thermodynamically unfavorable as the radius of the droplets fall and where the interfacial tension is similar to that at a planar surface. Interestingly, if the calculation were performed assuming the dependence of the interfacial tension on the curvature, the situation becomes more complex [3]. As shown in **Figure 2(b)**, with decrease in droplet radius from say, 1000 nm, there is an increase in interfacial free energy. But once the droplet becomes smaller below a certain radius, the interfacial free energy decreases and reaches a minimum value, before rising again with further decrease in radius. The interfacial free energy contribution still is the dominant factor, forcing the total free energy to attain a minimum value that is close to the optimum curvature of surfactant layer. Thus, under this consideration, one

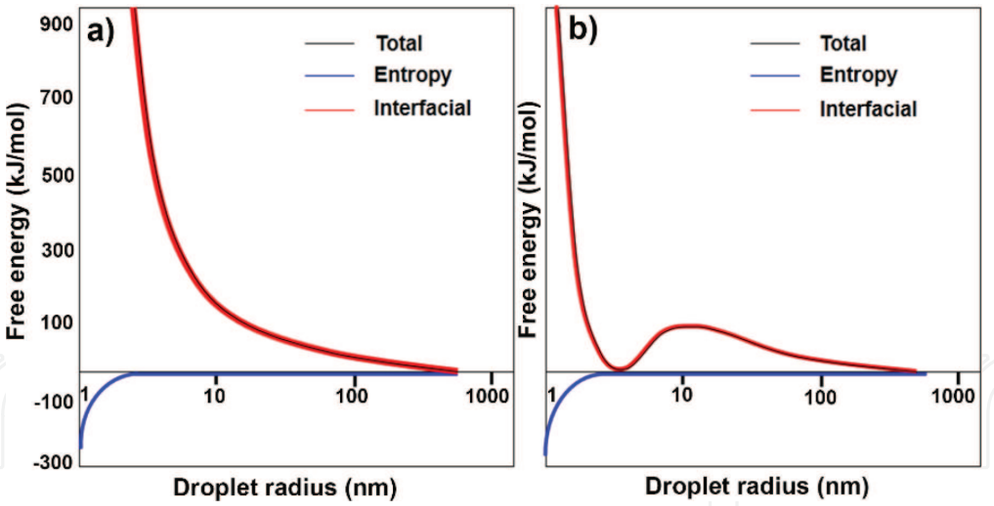

Figure 2.
Predicted variation of free energy change with droplet radius for the formation of emulsion state assuming (a) constant interfacial tension and (b) varying interfacial tension with curvature. Taken from Reference [3].

can assume that thermodynamically stable dispersion can be achieved when droplet radius is close to the optimum ($R = R_0$) and hence the interfacial free energy that otherwise opposes the emulsification can be appreciably reduced.

2.2 Kinetic picture

Kinetic stability, as to be contrasted with the thermodynamic stability, is determined by two important factors [3]: (1) Energy barriers: any energy barrier (or activation energy) that separates the two states (final and initial) will determine the rate of the conversion of one state to another. The height of this energy barrier depends on the forces operating in close proximity of two droplets, such as repulsive hydrodynamic and colloidal (steric and electrostatic) interactions [13]. Nanoemulsion can be made kinetically stable by introducing sufficiently large energy barrier (typically >20 kT) between the two states, while for microemulsion, there is still an activation energy required (in terms of mechanical agitation or heating the system) to reach the thermodynamically stable state after the components are brought into contact. (2) Mass transport phenomena: droplets in a nanoemulsion are particularly labile toward the growth over time by a process known as "Ostwald ripening" [8], in which solute molecules (or mass) are exchanged between the droplets via molecular diffusion through the solvent. Three alternative mechanisms have been proposed in the literature suggestive of that micelle which plays an important role in facilitating the mass exchange between the droplets by acting as carriers of oil molecules [8]. In mechanism *one*, oil molecules are transferred via direct micelle collisions, i.e., the rate is directly proportional to the volume fraction of micelle in solution. Numerous studies indicate a higher rate of mass transport above the CMC of the surfactant used. The lack of such CMC dependence for ionic surfactants however, may stem from the electrostatic repulsion between the droplet and micelle. In mechanism *two*, oil molecules exit the droplet, are exposed to the continuous phase and are soon captured by micelles in the immediate vicinity of the droplet. For non-ionic surfactant micelles, the higher rate of mass transfer is expected due to their higher solubilization capacity and the absence of electrostatic repulsion between the droplet and uncharged micelle. In mechanism *three*, a large number of oil molecules are released from the oil droplets collectively with excess of surfactant molecules to form a new micelle.

3. Formation of oil in water droplets from geometric and force balanced point of view

3.1 Role of surfactant in geometrical packing

We have already defined, in a limited sense, the word "surfactant" as an amphiphilic molecule which has the capacity to self-organize above a critical concentration. The process of self-assembly is dynamic in nature [13]. For those whose molecules at the air (or oil)-water interface are in exchange equilibrium with bulk solution are called soluble monolayer with a typical residence time on the order of 10^{-6} s. On the other hand, for those whose molecules are in less dynamic situation at the monolayer when the interface is expanded or compressed are called insoluble monolayer, and the time taken for such molecular exchange can vary typically from seconds to months (**Figure 3**).

The self-assembly of amphiphiles strongly depends on the two key surface forces that act at the interface: the "hydrophobic attraction" between the surfactant tails which induces the association of the molecules and the "hydrophilic repulsion" between the surfactant heads which helps them to remain in contact with water [13]. Though the selection of emulsifier in the preparation of either O/W or W/O nanoemulsions is still made on an empirical basis, however, a semiempirical scale is defined based on the relative percentage of hydrophilic to lipophilic groups in the surfactant molecules, known as hydrophilic-lipophilic balance (HLB number) [14], the HLB number is deduced from the preferential solubility of the surfactant in oil or water and HLB number can vary from 0 (very soluble in oil) to 20 (very soluble in water). Griffin postulated a simple equation to calculate the HLB number for non-ionic surfactant such as fatty acid ester [14], $HLB = 20 - \left(1 - \frac{S}{A}\right)$, where S is the saponification number and A is the acid number (**Figure 4**). Davies developed a method for calculating the HLB number for surfactants irrespective of their chemical nature, using empirically determined group numbers [15]: $HLB = 7 + \sum(\textit{hydrophilic group no}) - \sum \textit{lipophilic group no}$. Beerbower and Hills used the following expression for the HLB number [16]: $HLB = 20\left(\frac{M_H}{M_L + M_H}\right) = 20\left(\frac{V_H \rho_H}{V_L \rho_L + V_H \rho_H}\right)$, where M_H and M_L are the molecular weights of the hydrophilic and lipophilic portions of the surfactants. V_H and V_L are their corresponding molar volumes, whereas ρ_H and ρ_L are the respective densities. After adequately describing the interactions between the amphiphiles within an aggregate, we need to establish the

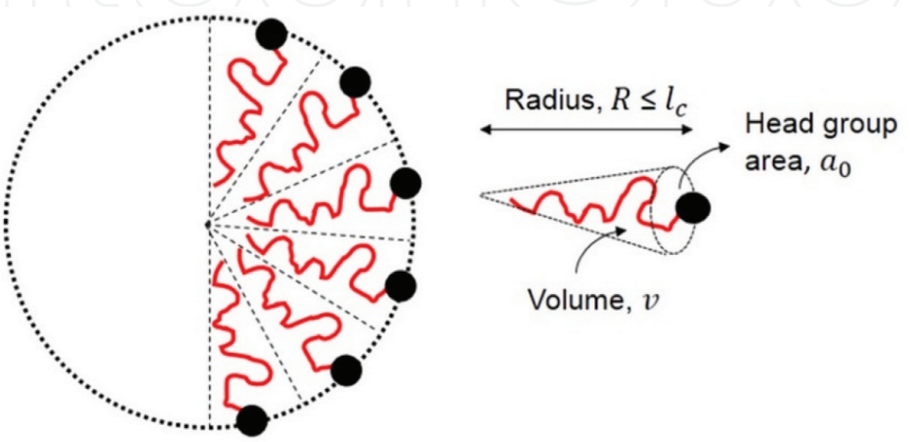

Figure 3.
Schematic representation of spherical micelle with illustration of different surfactant parameters. Packing factor = $\frac{V}{l_c a_0}$. The chain volume, v, and chain length l_c *set the aggregation limit.*

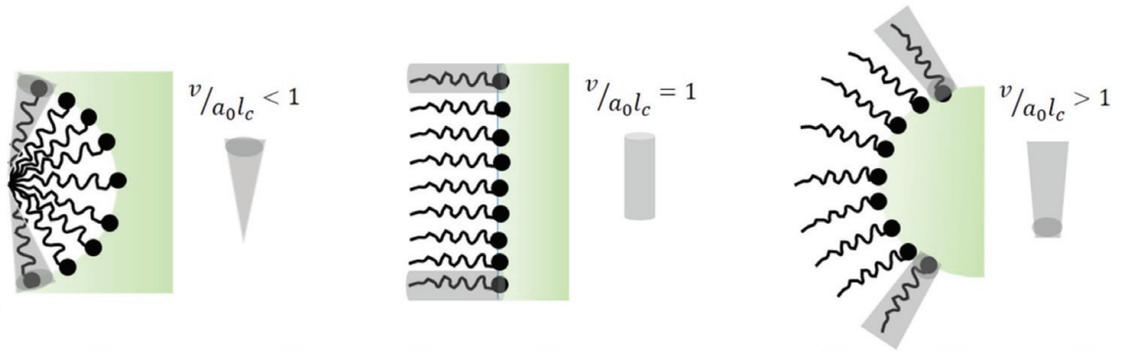

Figure 4.
View of the curvature of surfactant aggregates formed at various surfactant parameters, $\frac{v}{a_0 l_c}$. For less than one condition (left), the interface curves toward chain region. For greater than one condition (right), the interface curves toward the polar region. When exactly equal to one (middle), the interface exhibits no preferential curvature.

most favored structure of these aggregates. A convenient parameter to analyse such diverse structures is the dimensionless number, $v/a_0 l_c$, also known as "surfactant parameter" [17]. Close packing of amphiphiles leads to curved interfaces, and the direction of the curvature (either toward the polar or non-polar region) depends upon the value of this parameter. Here, l_c is a semiempirical parameter called the critical chain length of the same order (or somewhat less) as the fully extended molecular length of the chain, l_{max}; a_0 is the optimal head group area; and v is the volume of the hydrocarbon chain [17]. Once these parameters are specified for a given molecule, one may ascertain the most preferred geometrical packing. Gradation of the preferred structure with increasing surfactant parameter has been made as follows [13]: $v/a_0 l_c \leq \frac{1}{3}$ for spherical to $\frac{1}{3} \leq v/a_0 l_c \leq \frac{1}{2}$ for ellipsoidal to $v/a_0 l_c \approx \frac{1}{2}$ for cylindrical or rodlike micelle to $\frac{1}{2} \leq v/a_0 l_c \leq 1$ for various interconnected structures or lameller phases to $v/a_0 l_c = 1$ for vesicles or extended bilayer and finally to a family of "inverted structure" for $v/a_0 l_c > 1$. Therefore, it can be concluded that in a non-condensed liquid phase the curvature is a function of the surfactant parameter at the liquid-liquid interface. *Here, we find surface tension at work*, and consequently it *results in a pressure imbalance* across a curved surface [6]. The origin of the tendency to minimize the surface energy of oil droplets in water is due to the imbalance in forces acting on a molecule at the interface compared to those acting in the bulk. From the basic fluid dynamics, we find that when a surface is curved there is a difference in pressure on the two sides of the surface which is described by the very important concept of "Laplace pressure" on the two sides of a curved (non-planer) surface, a spherical one being a special case of this in general [6].

3.2 Derivation of Laplace equation

Consider a spherical cap symmetric about z-axis. The pressure exerted on the curved interface by the two bulk phases will be different and will give rise to a force acting along the normal to the interface at each point on the curve. The cap will also feel a force arising from surface tension acting tangentially at all points on the curve. At mechanical equilibrium, these two forces cancel each other along the z-direction (**Figure 5**).

Force arising from the pressure difference: $F_z^{\Delta P} = \left(P^{\alpha} - P^{\beta}\right) \sum \delta A = \left(P^{\alpha} - P^{\beta}\right) \pi r_c^2$.

Force arising from surface tension: $F_z^{\gamma} = \frac{2\pi r_c^2 \gamma}{r}$.

At equilibrium the forces along z-direction: $F_z^{\Delta P} = F_z^{\gamma}$; or $\left(P^{\alpha} - P^{\beta}\right)\pi r_c^2 = \frac{2\pi r_c^2 \gamma}{r}$.

So, $\Delta P = \left(P^{\alpha} - P^{\beta}\right) = \frac{2\gamma}{r}$, which is the *Laplace equation* for spherical surface.

For nonspherical interface, two orthogonal radii of curvature (r', r'') are needed, the *Laplace equation* then becomes $\Delta P = \gamma\left(\frac{1}{r'} + \frac{1}{r''}\right) = \frac{2\gamma}{r_m}$, where r_m is the mean curvature (inverse of radius) and is equal to $\frac{1}{r_m} = \frac{1}{2}\left(\frac{1}{r'} + \frac{1}{r''}\right)$. By our convention, if the interface encloses hydrophobic region, the mean curvature would be negative. Therefore, the Laplace pressure always drives the interface in the concave direction if the molecules are expanded or contracted. The high energy required for the formation of nanoemulsion droplets can be understood from the inverse relation of the pressure difference with the radius. The Laplace equation forms the theoretical basis of "Kelvin equation," which describes the effect of surface curvature of a liquid that changes with the equilibrium vapor pressure of the liquid [13]:

$\ln\left(\frac{P^c}{P^{\infty}}\right) = \left(\frac{2\gamma V_m}{r_m RT}\right)$, and we immediately obtain the *Kelvin radius*:

$r_k = \left(\frac{1}{r_1} + \frac{1}{r_2}\right)^{-1} = \frac{\gamma V_m}{RT\ln\left(\frac{P^c}{P^{\infty}}\right)}$, where P^c and P^{∞} are, respectively, the vapor pressures over the curved surface with mean curvature r_m and a flat surface ($r = \infty$), V_m is the molar volume of the oil, γ is the interfacial surface tension, R is the gas constant and T is the absolute temperature.

3.3 The consequences of Kelvin equation are profound

One of them is to govern the process such as the growth of larger droplet in expanse of the smaller one in nanoemulsion. The vapor pressure of a spherical droplet will be greater than that of the same liquid with a flat surface. *The smaller the radius, the higher the vapor pressure* such that if there is a distribution of droplet size, the smaller one will tend to diminish, while the larger ones will tend to grow. The total energy of the two-phase system thus can be decreased via an increase in the

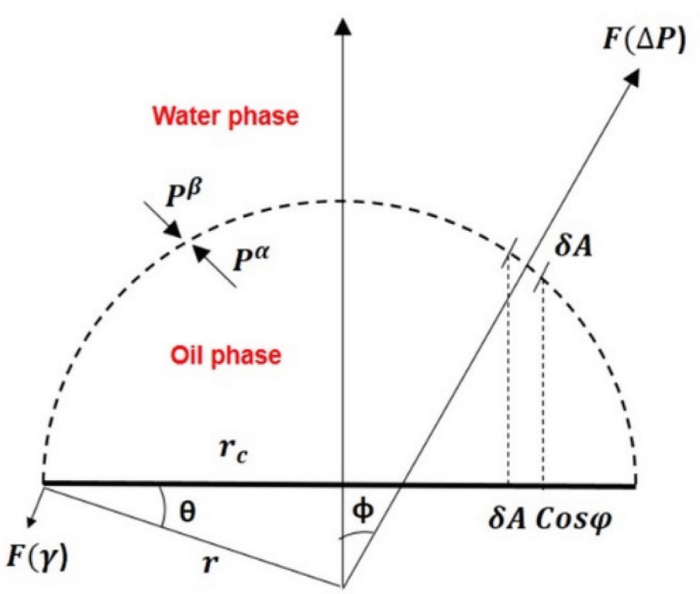

Figure 5.
Resolution of forces on spherical cap symmetrical about the z-axis and part of a spherical interface. The pressures exerted on the interface by the two bulk phases (α and β) will be different if the interface is curved, and this difference (ΔP) will give rise to a force acting along the normal to the interface at each point. The cap will also be subject to a force arising from surface tension acting tangentially at all points around the perimeter of the cap.

size scale of the second phase and accordingly a decrease in total interfacial area. Such a process is known as "Ostwald ripening." The driving force of the ripening process is the dependence of oil solubility on its size, as described by the Kelvin equation [18, 19]:

$$C(r) = C(\infty)\exp\left(\frac{2\gamma V_m}{RTr_m}\right) \approx C(\infty)\left(1 + \frac{2\gamma V_m}{RTr_m}\right),$$

where V_m is the molar volume of the oil and γ is the surface tension. This equation relates the solubility of droplet $C(r)$ with an arbitrary radius r to that of an infinite radius $C(\infty)$. The quantity $\left(\frac{2\pi V_m}{RTr_m}\right)$ has the dimension of length and is termed as the *capillary length* of the drop, typically on the order of ~1 nm. The Kelvin equation is derived from the dependence of chemical potential (μ) of the dispersed phase on its size by the relation [19]:

$$\Delta\mu(r) = \mu(r) - \mu(\infty) = \int_0^{2\gamma/r} V_m(p)dp \approx \frac{2\gamma V_m}{r}.$$

Another driving force for Ostwald ripening to occur in nanoemulsions is due to the polymorphic changes during redeposition of solute (such as drug molecules).

4. Theory of Ostwald ripening in nano-dispersion

So far, we came to know that the major instability of O/W nanoemulsions is caused due to the molecular exchange of oil molecules between droplets, a process known as *Ostwald ripening*. Although many specialists on emulsion stability are often unwilling to accept the concept of Ostwald ripening, instead, in most cases, they explain the destabilization under the framework of the more traditional mechanism—coalescence. Despite these disagreements in the literature, the theoretical development of the kinetic regime of the Ostwald ripening is a peculiar form of self-ordering and stimulates curiosity to the researchers till now. The detail mathematics of the theory of Ostwald ripening mechanism is not included in this chapter; rather, we will address a few selected topics of the theory. A more comprehensive discussion on this issue can be found in the reviews given in Refs. [19–21].

The major contribution in the theory of kinetics of Ostwald ripening in its contemporary form was initially formulated by Lifshitz and Slyozov [22] and then independently by Wagner [23] (known as LSW theory). Following publication of their findings, it became the seminal paper on which all subsequent theoretical works have been based. The theory is based on the following assumptions: (1) the particles (here droplets) of dispersed phase are spherical in shape, are fixed in space and are separated from each other by distance which are much larger than their sizes (true diluted system), (2) the mass transport is due only to the molecular diffusion through the dispersion medium and (3) the concentration of the molecularly dissolved species is constant except adjacent to the droplet boundaries.

4.1 Scaling the ripening problem

The ripening mechanism is characterized by two intervals, namely, the *transient* or short-time regime and the *asymptotic* limit or long-time regime. The transient limit is composed of a region of random variation of droplet size, whereas the

asymptotic limit ($t \to \infty$) is ascribed to the region that shows a linear relationship between the cubes of the number average droplet radius ($r_N{}^3$) with time.

We follow the procedure used in reference [21] by Kabalnov et al. If $f(r,t)$ be the size (radius) distribution function of the polydisperse system, such that $f(r,t)dr$ is the number of particles per unit volume in the size range r to $r + dr$. The change in the distribution function with time can be expressed as

$$\frac{df(t,r)}{dt} = 0,$$
$$\text{or } \frac{\delta f}{\delta t} + \frac{\delta f}{\delta r}\frac{dr}{dt} = 0,$$
$$\text{or } \frac{\delta f}{\delta t} + \frac{\delta}{\delta r}(f\dot{r}) = 0,$$

where $\dot{r} = \frac{dr}{dt}$ is the velocity of the particles

$$\text{i.e.} \frac{\delta f}{\delta t} + \frac{\delta j}{\delta r} = 0, \tag{1}$$

where $j = f\dot{r}$ is the flux of particles

Now, the growth rate of any droplet is proportional to its size, r, and the concentration, $C(t)$, of the substance of the droplet in the medium (which is a constant according to assumption 3) with respect to its equilibrium value, C_{eq} :

$$\text{i.e.} \frac{dV}{dt} \propto r\big(C(t) - C_{eq}(r)\big),$$
$$\text{or } \frac{4\pi}{3}\frac{d}{dt}r^3(t) = 4\pi D\, r\big(C(t) - C_{eq}(r)\big), \tag{2}$$

where D is the molecular diffusivity of the disperse phase in the medium.

$$\text{or } r^2\frac{dr}{dt} = Dr\big(C(t) - C_{eq}(r)\big); \text{ i.e.} \dot{r} = \frac{D}{r}\big(C(t) - C_{eq}(r)\big).$$

Now, we introduce a dimensionless quantity θ, which is a measure of the relative concentration by $\theta(t) = \left(\frac{C(t)-C_{eq}(\infty)}{C_{eq}(\infty)}\right)$; now from the Kelvin equation, we know that $C_{eq}(r) = C_{eq}(\infty)\big(1 + \frac{\alpha}{r}\big)$.

Therefore, $\dot{r} = \frac{D}{r}\big(C(t) - C_{eq}(\infty)\big(1 + \frac{\alpha}{r}\big)\big)$.

Rearranging the equation we get

$$\dot{r} = \frac{DC_{eq}(\infty)}{r}\left(\left(\frac{C(t) - C_{eq}(\infty)}{C_{eq}(\infty)}\right) - \frac{\alpha}{r}\right),$$
$$\text{or } \dot{r} = \frac{DC_{eq}(\infty)}{r}\left(\theta(t) - \frac{\alpha}{r}\right). \tag{3}$$

This is the expression of velocity of particle in size space. The value of particle radius at which the growth rate at any instant of time is zero ($\dot{r} = 0$) is called the instantaneous critical radius (r_c); then, it is obvious that $r_c = \alpha/\theta(t)$, and for growth rate equation, we can write $\theta(t) - \frac{\alpha}{r} > 0$ or $\frac{\alpha}{r} < \theta(t)$ or $r > \frac{\alpha}{\theta(t)}$, i.e. $r > r_c$, which means that at any instance of time particle with radius greater than the critical radius will exhibit an increase in size where the particle having radius smaller than the critical

one will become smaller (decay). In this notation the growth rate equation (Eq. (2)) can be rewritten as follows:

$$\frac{4\pi}{3}\frac{d}{dt}r^3(t) = 4\pi D\, C_{eq}(\infty)\alpha\left(\frac{r}{r_c} - 1\right),$$

$$\text{or } \dot{r} = \frac{DC_{eq}(\infty)}{r^2}\left(\frac{r}{r_c} - 1\right).$$

The final element of LSW theory is the mass conservation.

In a closed system, the concentration of a substance in the medium and the drop size distribution function is interrelated by

$$\frac{d}{dt}\left[C(t) + \frac{4\pi}{3}\int_0^\infty r^3 f(r,t)dr\right] = 0,$$

$$\text{or } \theta(t) + \frac{4\pi}{3C_{eq}(\infty)}\int_0^\infty r^3 f(r,t)dr = \theta(0). \tag{4}$$

The three integro-differential Eqs. (1), (3) and (4) can be solved analytically. It was shown that this system should have an asymptotic solution which is independent of initial conditions. Rather than solving the problem for all times, LSW found an asymptotic solution valid as t → ∞. Using this approach, the following predictions were made for two-phase mixture undergoing Ostwald ripening in the long-time limit [20]:

1. Time evolution of average droplet radius: $\overline{R}(t) = \left(\overline{R}^3(0) + 4t/9\right)^{1/3}$

2. Time evolution of the number of droplets per unit volume:
   $N(t) = \psi\left(\overline{R}^3(0) + 4t/9\right)^{-1}$

3. Time invariant droplet size distribution function: $f\left(\overline{R},t\right) = \frac{g(u)}{\overline{R}^4}$

where depending on the approach, $\overline{R}$ is either the critical radius (r_c) or the maximum drop size; $\overline{R}(0)$ is the average radius at the onset of coarsening; $\psi = \theta/\alpha\int_0^{3/2} u^3 g(u)du$, θ is the dimensionless concentration, $\theta = (C - C(\infty))/C(\infty)$; and u is the normalized radius, $u = R\overline{R}$, $\alpha = 4\pi/(3V_m C(\infty))$.

The *salient results of LSW theory* are summarized as follows:

1. In the stationary region, the nature of the size distribution function is time invariant.

2. The cube of the number-averaged particle size (r_N) varies linearly with time:

$$\omega = \frac{d}{dr}\left(r_N{}^3\right) = \left(\frac{8\gamma DC(\infty)V_m}{9RT}\right) = \frac{4}{9}\alpha DC^\infty,$$

where r_c is the radius of droplet at steady state, D is the diffusion coefficient of the dispersed phase in the continuous phase and α is the characteristic length scale ($\alpha = 2\gamma V_m/RT$). Droplet with radius $r < r_c$ will disappear, while droplet with $r > r_c$ will grow.

The comparison between theoretical and experimental Ostwald ripening rates, however, evoked a significant discrepancy in the literature [18], where the latter was found to be several times higher than the former. It has been found that the linear relation of $r_N{}^3$ with time in the asymptotic limit does not always signify the Ostwald ripening; as a second mechanism, "Brownian-induced coalescence" (particularly if the drop surface coverage is not sufficient to hinder the coalescence) may also be operative, which has the same dependency of the rate over time. The LSW theory assumed that the droplets are fixed in space and the molecular diffusion is the only mechanism of mass transfer. However, for the case of droplets undergoing Brownian motion, one must take into account both the contribution of molecular and convection diffusion as predicted by Peclet number (P_e = rv/D). The velocity v of a droplet of mass M is approximately given by $v = \left(\frac{3kT}{M}\right)^{1/2}$.

4.2 Adjustment in Ostwald ripening rate

The rate of ripening, according to the LSW model, is directly proportional to the solubility of the oil in the aqueous medium. The presence of amphiphiles (surfactants or co-surfactants) can significantly enhance the oil solubility by allowing them to enter into their hydrophobic core. By replacing the bulk solubility of oil, $C(\infty)$ by the concentration of oil solubilized by the micelles, and using the micellar diffusion coefficient instead of the molecular diffusion, one would get the Ostwald ripening rate in the presence of micelle. According to the *extended LSW theory*, the Ostwald ripening rate of nanoemulsion containing a water-insoluble low molecular weight coemulsifier (amphiphile) can be predicted by the following equation [24], $\omega = \left(\frac{64\gamma D_{co} C_{co}(\infty) V_m}{9RT}\right)\phi_{co}$, where D_{co}, $C_{co}(\infty)$ and ϕ_{co} are the molecular diffusivity, bulk solubility (in water) and volume fraction of the coemulsifier in the oil droplet, respectively. Similarly, as the interfacial tension (γ) is incorporated in the ripening rate equation in the capillary length parameter (α = $2\gamma V_m$/RT), lowering of the interfacial tension by the amphiphiles will lead to smaller capillary length and therefore lower solubility of the oil at the droplet boundary. This will cause lowering of the ripening rate at least for the case of strongly adsorbed amphiphiles. In the absence of micelle, oil molecule transports into and through the aqueous phase separating the droplets. However, in the presence of micelle, it is proposed that mass transfer is still involved through the continuous phase, but the micelles increase the water solubility of the oil, therefore effectively increasing the transport rate [24–26]. Kabalnov [19] has proposed three possible mechanisms to explain the observed effects of micelles on Ostwald ripening; nevertheless, whether the oil molecules are taken up by the micelles directly from the aqueous medium or by fusion/fission of a micelle with a droplet surface is still unclear. Another possible way to slow down the Ostwald ripening rate was proposed by Higuchi and Misra [27] through the incorporation of a second disperse phase (oil) with a much lower continuous phase solubility. Initially, the concentration of the second insoluble phase is equal in all droplets. As the mixed oil nanoemulsion undergoes Ostwald ripening, the more soluble component diffuses from the smaller to larger droplet at a much faster rate than the less soluble one. Thus, time will come when the larger droplets become enriched with the soluble oil and the chemical potential of that component is equal in all the droplets. Thus, there is no driving force for further transfer of the oil to take place, and the state is referred to as pseudo-steady of ripening. As theoretically investigated by Kabalnov et al. in the case of medium-soluble second component, the Ostwald ripening rate of the mixed oil nanoemulsion can be approximated as [25]

$$\omega_{mix} = \left(\frac{\phi_1}{\omega_1} + \frac{\phi_2}{\omega_2}\right)^{-1},$$

where ϕ_1 and ϕ_2 and the ω_1 and ω_2 are the volume fraction and ripening rate of the medium-soluble and medium-insoluble component, respectively. In his treatment [25], Kabalnov came up with three stability regime depending on the mole fraction of the less soluble second component (X_2) in the mixture. For high amount of insoluble oil ($X_2 > 0.4$), entropy of mixing dominates, $\Delta\mu < 0$, and the nanoemulsion is thermodynamically stable. For low mole fraction ($X_2 < 0.17$), Laplace pressure between the different size droplets dominates, and the nanoemulsion is thermodynamically unstable. At intermediate mole fraction ($0.17 < X_2 < 0.4$), a nanoemulsion is said to be in metastable state. Initially, Laplace pressure will dominate and the system undergoes Ostwald ripening; however, it also has a kinetic energy barrier that prevents further ripening to occur.

The validity of the LSW theory was tested by Kabalnov et al. [18, 19]. The influence of the alkyl chain length of the hydrocarbon on the Ostwald ripening rate of nanoemulsion was systematically investigated from alkyl chain length C9–C16. Increasing the alkyl chain length of the hydrocarbon used for the emulsion results in the decrease in the oil solubility. According to the LSW theory, this reduction in solubility should result in a decrease in the Ostwald ripening rate which was confirmed by Kabalnov et al.

5. Stability against coalescence in nano-dispersion

Though the droplets coalescence rate is sufficiently get reduced for the nanoemulsion due to their smaller size, however, as a consequence of Ostwald ripening, it may results in creaming and ultimately leads to phase separation of the nanoemulsion (**Figure 6a**). The importance of droplet deformation, surfactant transfer and interfacial rheology for the stability of emulsion is well reported in the literature [28–30]. In the presence of thermal noise, the droplets are allowed to explore space by Brownian motion, and the resulting collisions cause the mean droplet radius R to increase. This process is called *coalescence*. Stabilization against

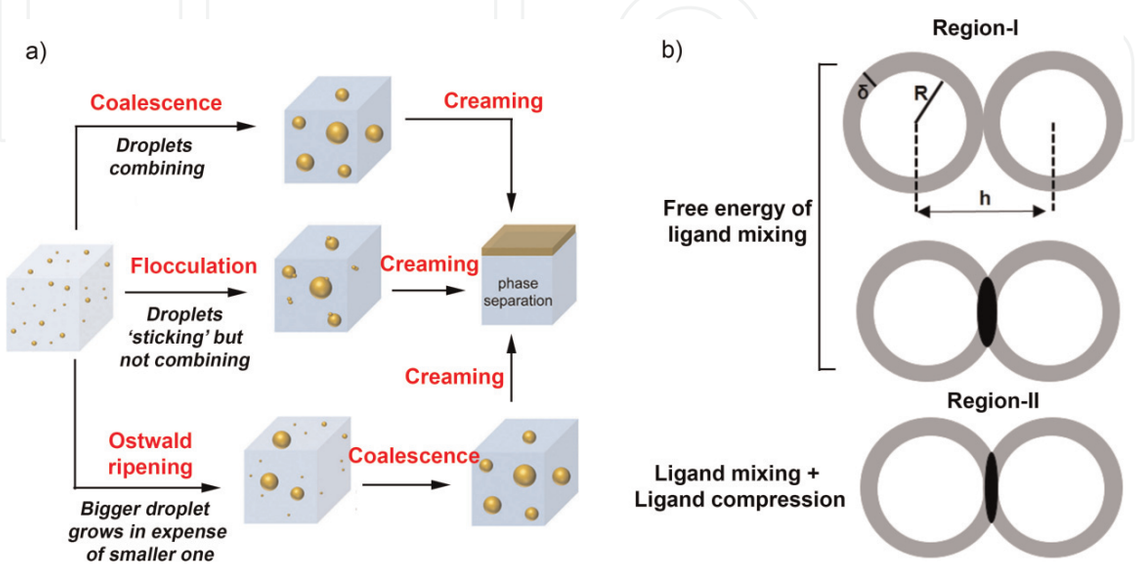

Figure 6.
(a) Schematic elaboration of various destabilization mechanisms for nanoemulsion and (b) cartoon of drop-drop interaction under two different regions where ligand shell overlaps each other.

coalescence can be effectively achieved, by creating a sufficient repulsive energy barrier between the droplets. This can be done by two ways, such as for O/W nanoemulsion the *electrostatic* stabilization (due to creation of double layer) by adding ionic surfactants. The formation of an electrical double layer (EDL, thickness δ) barrier is well established in the literature of colloidal stability according to the Derjaguin, Landau, Verwey and Overbeek (DLVO) theory [31]. As a result of this EDL formation when droplets approach a distance h, smaller than twice the double layer extension, strong repulsion occurs against their aggregation; hence, flocculation is prevented. A second and more effective mechanism using non-ionic surfactants or polymer (referred as surfactant) for W/O nanoemulsion is the *steric* stabilization (due to the presence of adsorbed polymer layer). However, no comparable definitive theory exists till date for the so-called steric stabilization. To date there have been several attempts made to develop the quantitative theory of steric stabilization with a notable success of *Fischer's solvency theory* [32] which exploits the Flory-Huggins theory [33] to predict the repulsive potential energy between two large flat plates. The total free energy of interaction obtained by Hesselink et al. for two flat plates coated by steric layer is given by [33]

$$\frac{U_{total}}{kT} = (2\pi/9)^{\frac{3}{2}}\gamma^2(\alpha^2 - 1)r_{rms}M(d) + 2\gamma V(d),$$

where γ is the number of ligands per unit area, α is the expansion factor, r_{rms} is the root mean square end-to-end distance of the chain in free solution and $M(d)$ and $V(d)$ are the distance-dependent mixing and elastic function that could be evaluated from segment density distribution function. However, the reason for the failure of Fischer's solvency theory appears to reside in the use of segment density distribution functions relevant to the isolated polymer according to Hesselink calculation [34] which is found unlikely to be applicable here. Smitham, Evans and Napper first pointed out the correction and proposed a simple analytical model to adopt for the segment density distribution function which is a constant segment density step function [35]. Their theory is able to account for many of the qualitative and quantitative features of steric stabilization observed to date. According to this model, the steric repulsion appears from two main origins: the *first one* (**Figure 6b**) is the unfavorable mixing of the surfactant chains which depends on their density at the interfacial region, on thickness of the interfacial layer (δ) and on the Flory-Huggin parameter, χ. The *second one* (**Figure 6b**) is the reduction in configuration entropy due to elastic stress of the chains which occur when inter-droplet distance becomes lower than δ. This method of stabilization is more effective than electrostatic stabilization in two ways: firstly, the repulsion is still maintained at moderate electrolyte concentration, and, secondly, the repulsion can be maintained at high temperature (provided ligand has solubility at that temperature).

The unfavorable mixing of the surfactant chains (considering the chain-solvent interaction predominates over the chain-chain interaction, like it is in good solvent condition) occurs when the ligand chain starts to interpenetrate within a distance, $1 + \overline{L} < h < 1 + 2\overline{L}$, where $\overline{L}$ is the rescaled length of ligand chain $\left(\overline{L} = \frac{\delta}{d}\right)$, δ is the contour length and $d(=2R)$ is the diameter of the sphere. The free energy of mixing in terms of rescaled parameter can be expressed as [35]

$$\frac{U_{mix}}{kT} = \frac{\pi d^3}{2V_{sol}^M}\varphi_{lig}^2\left(\frac{1}{2} - \chi\right)\left(h - \left(1 + 2\overline{L}\right)\right)^2; \text{when, } 1 + \overline{L} < h < 1 + 2\overline{L},$$

where V_{sol}^M, φ_{lig}, χ and h are the molar volume of the solvent, the average volume fraction of the ligand segments in the overlapping region, the Flory-Huggin

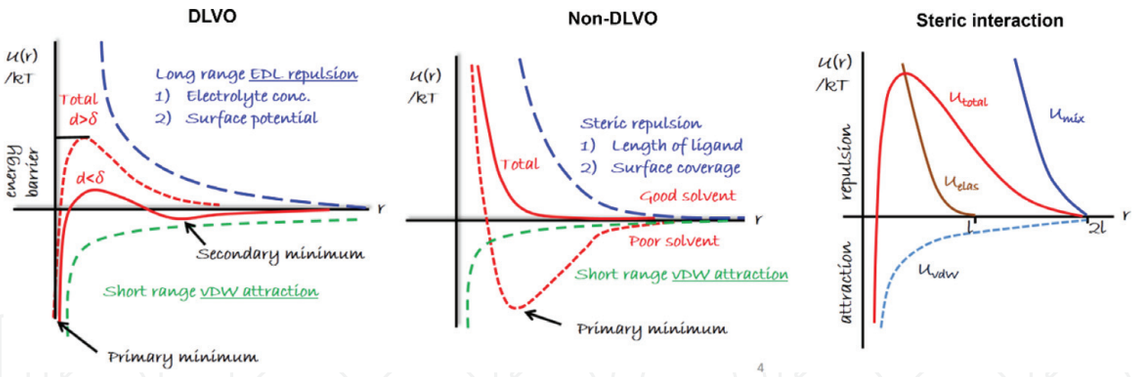

Figure 7.
Pictorial representation of distance dependence of pair potential energy between two spheres according to the literature.

interaction parameter and the center-to-center distance between any two approaching spheres, respectively. When $\chi < 0.5$, G_{mix} is positive and the interaction is repulsive. When $\chi > 0.5$, G_{mix} is negative and the interaction is attractive. When $\chi = 0.5$, G_{mix} is zero, which is referred to as the θ–condition. The Flory-Huggin parameter is calculated by $\frac{V_m}{RT}(\delta_s - \delta_m)^2 + 0.34$, where δ_s and δ_m are the Hildebrand solubility parameters [36] of the surfactant and solvent, respectively. Solubility parameter δ_2 of any component is related to its heat of vaporization ΔH with molar volume by $\delta_2 = \frac{\Delta H - RT}{V_m}$.

Continuing on the droplet-droplet approach within a distance $h < 1 + \overline{L}$, a second regime appears where chains undergo significant interpenetration and compression. The free energy of mixing in this regime can be expressed as [37]

$$\frac{U_{mix}}{kT} = \frac{\pi d^3}{2V_{sol}^M}\varphi_{lig}^2\left(\frac{1}{2} - \chi\right)\left[3\ln\left(\frac{\overline{L}}{h-1}\right) + 2\left(\frac{h-1}{\overline{L}}\right) - \frac{3}{2}\right], \text{ when } h < 1 + \overline{L},$$

while the elastic interaction U_{el} between the surfactant tails resulting from the loss in configurational entropy in this region is given by the expression [35]

$$\frac{U_{el}}{kT} = \pi\gamma d^2\left[(h-1)\left(\ln\frac{h-1}{\overline{L}} - 1\right) + \overline{L}\right]; \text{when, } h < 1 + \overline{L},$$

where γ is the number of ligands per unit area of the sphere. Therefore, U_{el} is always repulsive (**Figure 7**). A pictorial representation of pair potential vs. inter-particle distance was shown in **Figure 7** elaborating various cases of DLVO and non-DLVO interactions.

Therefore, the *criteria for effective steric stabilization* are the following: (1) the particle should be completely covered by the polymer, (2) the polymer should be strongly adsorbed to the particle surface, (3) the stabilizing chain should be highly soluble in the medium and is strongly solvated by its molecules and (4) δ should be sufficiently large to prevent weak flocculation which occurs when the thickness of adsorbed layer becomes small (<5 nm).

6. Conclusion

This chapter summarizes the most important aspects of nanoemulsion including the composition, structure and physical properties and also provides the glimpses of

trademarks which distinguished it from the conventional microemulsion. Droplets having dimension in the order of few tens of nanometers are unstable due to the high difference in vapor pressure outside and inside the curved interface. The presence of polydispersity in the droplet size leads to the difference in their chemical potential (and hence solubility), which acts as a fuel for the transfer of mass between two droplets. However, with the help of a proper stabilizing layer of polymer (favorable volume to [head group area $\times$ length] ratio) or surfactant, we can achieve the necessary repulsive barrier (electrostatic, steric or electro-steric) against their coalescence. Concurrently though, it also raises the question of whether the additive (surfactant or polymer) can affect the rate of Ostwald ripening during the mass transfer process. With the proper knowledge of the surfactant properties (HLB and other surfactant parameters), one can effectively fabricate a stable nano-dispersion for a particular combination of dispersed and continuous phase.

7. Outlook

In order to leverage the knowledge of structure-property-function relationship for nanoemulsion, a continuous effort in research and development is required in this direction. The recent advances in nanoemulsion fabrication with reduced polydispersity in droplet size distribution are likely to provide new avenue to the researcher for achieving their desired functionality. Indeed, we are not so far to fabricate smart nanoemulsion (decorated, functionalized and internally structured) which can act as a vaccine or drug delivery vehicle to provide enhanced therapeutic response to biological system. Molecular design of amphiphiles can lead to new stable nanoemulsion topologies such as double nanoemulsion. Aggregate/gel can be formed by attractive nanoemulsion droplets by introducing strong opposite screening layer, or elastic verification in the system of repulsive nanoemulsion can be made through high-flow emulsification that cause extreme droplet rupturing.

Overall, nanoemulsions are very promising and flexible soft-matter systems, and they offer outstanding potential for new advances in basic science, customized colloidal design and high-value applications.

Acknowledgements

This material is based upon the work supported by the Science and Engineering Research Board (SERB), Department of Science and Technology, India. The author would like to thank Dr. B.L.V. Prasad.

DOI: http://dx.doi.org/10.5772/intechopen.84201

IntechOpen

Author details

Kaustav Bhattacharjee
CSIR-National Chemical Laboratory, Pune, India

*Address all correspondence to: kaustavbhattacharjee@gmail.com

References

[1] Emulsions: Formation, Stability, Industrial Applications, by Tharwat F. Tadros, 2016. Walter de Gruyter GmbH, Berlin/Boston. e-ISBN (PDF) 978-3-11-045224-2

[2] Emulsion Science: Basic Principles An Overview, by Bibette J, Leal-Calderon F, Schmitt V, Poulin P. Springer-Verlag Berlin, Heidelberg, New York. ISSN electronic edition: 1615-0430

[3] McClements DJ. Nanoemulsions versus microemulsions: Terminology, differences, and similarities. Soft Matter. 2012;**8**:1719-11729. DOI: 10.1039/C2SM06903B

[4] Anton N, Vandamme TF. Nano-emulsions and micro-emulsions: Clarifications of the critical differences. Pharmaceutical Research. 2011;**28**: 978-985. DOI: 10.1007/s11095-010-0309-1

[5] Gupta A, Eral HB, Hatton TA, Doyle PS. Soft Matter. 2016;**12**:2826-2841. DOI: 10.1039/C5SM02958A

[6] Lautrup B. Physics of Continuous Matter. 2nd ed. Boca Raton: CRC press; 2011. DOI: 10.1080/00107514.2012.756936

[7] Tadros TF. Applied Surfactant: Principles and Application. Weinheim: Wiley; 2005. DOI: 10.1002/3527604812

[8] Tadros TF. Nanodispersions. Berlin/Boston: de Gruyter GmbH; 2016

[9] Wennerstrom H, Balogh J, Olsson U. Interfacial tensions in microemulsions. Colloids and Surfaces A: Physicochemical and Engineering Aspects. 2006;**291**: 69-77. DOI: 10.1016/j.colsurfa.2006.09.027

[10] Evilevitch A, Jonsson BT, Olsson U, Wennerstrom H. Molecular transport in a nonequilibrium droplet microemulsion system. Langmuir. 2001;**17**:6893-6904. DOI: 10.1021/la010899d

[11] Evilevitch A, Olsson U, Jonsson B, Wennerstrom H. Kinetics of oil solubilization in microemulsion droplets. Mechanism of oil transport. Langmuir. 2000;**16**:8755-8762. DOI: 10.1021/la000511z

[12] Hunter RJ. Foundations of Colloid Science. 2nd ed. Vol. II. London: Clarendon Press; 1989

[13] Israelachvili J. Intermolecular and Surface Forces. 2nd ed. Massachusetts: Academic Press; 1995

[14] Griffin WC. Classification of surface-active agents by HLB. Journal of the Society of Cosmetic Chemists. 1949; **1**:311 97

[15] Davies JT, Rideal EK. Interfacial Phenomena. 2nd ed. Massachusetts: Academic Press; 1963

[16] Beerbower A, Hill MW. Application of cohesive energy ratio (CER) concept to anionic surfactants. American Cosmetics and Perfumery. 1972;**87**: 85-94

[17] Hyde S, Andersson S, Larsson K, Blum Z, Landh T, Lidin S, et al. The Language of Shapes: The Role of Curvature in Condensed Matter: Physics, Chemistry and Biology. 1st ed. Amsterdam: Elsevier; 1997

[18] Kabalanov AS, Makarov KN, Pertsov AV, Shchukin ED. Ostwald ripening in emulsions: 2. Ostwald ripening in hydrocarbon emulsions: Experimental verification of equation for absolute rates. Journal of Colloid and

Interface Science. 1990;**138**:98-104. DOI: 10.1016/0021-9797(90)90184-P

[19] Kabalanov AS. Ostwald ripening and related phenomena. Journal of Dispersion Science and Technology. 2001;**22**:1-12. DOI: 10.1081/DIS-100102675

[20] Voorhees P. The theory of Ostwald ripening. Journal of Statistical Physics. 1985;**38**:231-252. DOI: 10.1007/BF01017860

[21] Kabalnov AS, Shchukin ED. Ostwald ripening theory: Applications to fluorocarbon emulsion stability. Advances in Colloid and Interface Science. 1992;**38**:69-97. DOI: 10.1016/0001-8686(92)80043-W

[22] Lifshitz IM, Slyozov VV. The kinetics of precipitation from supersaturated solid solutions. Journal of Physics and Chemistry of Solids. 1961;**19**:35-50. DOI: 10.1016/0022-3697(61)90054-3. (Translated by Lowde RD)

[23] Wagner C. Theory of the aging of precipitation by redissolution (Ostwald ripening). Zeitschrift für Elektrochemie. 1961;**65**:581-591. DOI: 10.1002/bbpc.19610650704

[24] Kabalnov AS. Can micelles mediate a mass transfer between oil droplets? Langmuir. 1994;**10**:680-684. DOI: 10.1021/la00015a015

[25] Kabalnov AS, Pertsov AV, Shchukin ED. Ostwald ripening in two-component disperse phase systems: Application to emulsion stability. Colloids and Surfaces. 1987;**24**:19-32. DOI: 10.1016/0166-6622(87)80258-5

[26] Smet YD, Deriemaeker L, Finsy R. Ostwald ripening of alkane emulsions in the presence of surfactant micelles. Langmuir. 1999;**15**:6745-6754. DOI: 10.1021/la9901736

[27] Higuchi WI, Misra JJ. Physical degradation of emulsions via the molecular diffusion route and the possible prevention thereof. Journal of Pharmaceutical Sciences. 1962;**51**:459-466. DOI: 10.1002/jps.2600510514

[28] Ivanov IB, Danov KD, Kralchevsky PA. Physical degradation of emulsions via the molecular diffusion route and the possible prevention thereof. Colloids and Surfaces A: Physicochemical and Engineering Aspects. 1999;**152**:161-182. DOI: 10.1016/S0927-7757(98)00620-7

[29] Petsev DN, Denkov ND, Kralchevsky PA. Flocculation of deformable emulsion droplets. Journal of Colloid and Interface Science. 1995;**176**:201-213. DOI: doi.org/10.1006/jcis.1995.0023

[30] Denkov ND, Petsev DN, Danov KD. Flocculation of deformable emulsion droplets. I. Droplet shape and line tension effects. Journal of Colloid and Interface Science. 1995;**176**:189-200. DOI: 10.1006/jcis.1995.0022

[31] Verwey EJ, Overbeek JTG. Theory of the Stability of Lyophobic Colloids. 1st ed. Amsterdam: Elsevier; 1948

[32] Fischer EW. Electron microscopic studies on the stability of suspensions in macromolecular solutions. Kolloid-Zeitschrift. 1958;**160**:120-141. DOI: 10.1007/BF01512392

[33] Flory J. Principles of Polymer Chemistry. Ithaca: Cornell University Press; 1953

[34] Hesselink FT, Vrij A, Overbeek JTG. Theory of the stabilization of dispersions by adsorbed macromolecules. II. Interaction between two flat particles.

Journal of Physical Chemistry. 1971;**75**: 2094-2103. DOI: 10.1021/j100683a005

[35] Smitham JB, Evans R, Napper DH. Analytical theories of the steric stabilization of colloidal dispersions. Journal of the Chemical Society, Faraday Transactions. 1975;**1, 71**: 285-297. DOI: 10.1039/F19757100285

[36] Hildebrand JH. Solubility of Non Electrolytes. 2nd ed. New York: Reinhold; 1936

[37] Evans R, Smitham JB, Napper DH. Theoretical prediction of the elastic contribution to steric stabilization. Colloid & Polymer Science. 1977;**255**: 161-167. DOI: 10.1007/BF01777275